# MRI Characterization of Iron in Soluble (Ferritin-like) and Particulate (Hemosiderin-like) Mixtures

**J. S. Cheung[1,2], A. M. Chow[1,2], J. H. Jensen[3], H. Tang[4], T. R. Brown[5], S. Sheth[6], G. M. Brittenham[6], and E. X. Wu[1,2]**

[1]Laboratory of Biomedical Imaging and Signal Processing, The University of Hong Kong, Pokfulam, Hong Kong, [2]Department of Electrical and Electronic Engineering, The University of Hong Kong, Pokfulam, Hong Kong, [3]Department of Radiology, New York University, New York, New York, United States, [4]Department of Imaging, Merck Research Laboratories, Rahway, New Jersey, United States, [5]Department of Radiology, Columbia University, New York, New York, United States, [6]Department of Pediatics, Columbia University, New York, New York, United States

## INTRODUCTION

Accurate MRI characterization of tissue iron is needed to improve the diagnosis and management of patients with iron overload, including thalassaemia major, hereditary hemochromatosis, aplastic anemia, myelodysplasia and other disorders[1]. In patients with iron overload, virtually all of the excess iron is sequestered within cells as short-term storage iron in ferritin (soluble nanometer-sized particles, dispersed and relatively uniformly distributed) and as long-term iron deposits in hemosiderin (insoluble and clumped in irregular micron-sized clusters separated by distances of 10 to 30 μm[2]). We hypothesize that the readily mobilizable ferritin iron is in closer equilibrium with the toxic low molecular weight iron pool responsible for cellular injury than is the long-standing reserve in hemosiderin. A variety of MRI techniques have been developed[3] to assess tissue iron deposition. Almost all are based on the simple measurement of bulk $R_2$* and $R_2$ to provide estimates of *total* storage iron and are not adequate to separately determine the amounts of ferritin and hemosiderin iron. The differences in solubility and spatial distribution between ferritin and hemosiderin are reflected in their distinct effects on MR signal decay. Ferritin iron affects MRI signal decay principally through a proton exchange mechanism[4] while hemosiderin primarily produces magnetic field inhomogeneities and causes large susceptibility effects. Jensen and Chandra first formulated a theory of the effects of particulate iron on modified multi-echo CPMG signal decay[5]. Their theory has been applied to study tissue iron overload[6] but formal experimental validation of the approach is lacking. The overall aim of our study was to determine experimentally whether ferritin and hemosiderin iron can be differentiated by conducting MRI study of phantoms that contain soluble ferritin-like iron and particulate hemosiderin-like iron within cells.

## METHODS

Theory: In brief, the non-exponential MR signal decay in an uniform suspension of soluble iron and particulate iron is predicted to approximately follow the analytical form[5,6]: $S(TE) = S_0 e^{-RR_2 \times TE} e^{-[A^{3/4}(\Delta t)^{3/4}(TE - t_s)^{3/8}]}$ where $t_s = 2\tau[1-(\tau/\Delta t)^2]$. $2\tau$ is the first echo time, $2\Delta t$ interecho time, TE echo time. Parameter $A$ is predominately determined by large particles of strong magnetic susceptibility or hemosiderin iron, and designated as the "hemosiderin index". $RR_2$, the reduced transverse relaxation rate, is primarily sensitive to ferritin iron and termed the "ferritin index".

Phantoms: Two types of phantoms were employed to experimentally validate the formulation above. (**1**) To mimic the intracellular and irregularly- shaped hemosiderin chunks in iron overload tissue, phantoms were constructed using agarose gel suspensions of iron-loaded cells (mouse embryonic stem cells or ESCs and human embryonic kidney cells or HEKs). ESCs and HEKs were intracellularly loaded with aggregated iron oxide particle clusters or chunks (monocrystalline iron oxide nanoparticles or MIONs at about 2-4 pg Fe/cell in ESCs; 0.9 μm superparamagnetic micron-sized particles of iron oxides or MPIOs at about 3-10 pg Fe/cell in HEKs) using a procedure developed for MRI cell labeling via endocytosis. Cell concentrations were varied in different phantoms to mimic different hemosiderin concentrations. Cell viabilities were confirmed by Trypan blue before suspending cells in gel. (**2**) Phantoms were also constructed of uniform suspensions of soluble superparamagnetic monocrystalline iron oxide nanoparticles (MION) and insoluble 4.5 μm MPIOs in agarose gel with various MION and MPIO concentrations.

MRI Experiments: Modified multi-echo CPMG imaging sequences were implemented and optimized on a 7T Bruker scanner to measure the MR signal decays in these phantoms. A short first echo time $2\tau$ (3-4ms) was used to sample the initial rapid drop in the decay curve effectively. 11 or 7 interecho times ($2\Delta t$, 4–24 ms for cell phantoms and 4–16 for iron oxide phantoms) were employed to provide robust fitting to the equation above for the "ferritin" index $RR_2$, "hemosiderin" index $A$, and $S_0$. MRI signal decay data from ROI in each phantom was used for least square fitting.

## RESULTS

As shown in Fig. 1, close linear correlations ($R^2 > 0.98$) were found in each phantom set between the particulate iron (MPIO or iron loaded inside the cells) concentrations and $A^{3/4}$ values, and between the soluble iron (MION) concentrations and $RR_2$ values. These experimental results indicated the robustness of this CPMG approach to separately determining $RR_2$ and $A$. The minor discrepancies in Figure 1 likely result from imperfections in phantom preparations (e.g., concentration and MPIO particle or cell distribution uniformity; presence of air-bubbles).

## CONCLUSIONS AND DISCUSSIONS

The phantom results of our study provide a compelling experimental validation of the theoretical formulation of Jensen and Chandra[5] and demonstrate the ability of this approach to discriminate between soluble and particulate iron. The theory is shown to be robust for iron particles, in both spherical and irregularly-clustered forms. Our results suggest that this approach can be used to characterize the ferritin and hemosiderin iron separately in iron overloaded tissue such as liver and myocardium. Although the ferritin-like iron index $RR_2$ and hemosiderin-like iron index $A$ here are not calibrated and translated to the absolute iron content here, such indices are potentially valuable in monitoring transfusion-dependent thalassaemia major patients and assessing iron toxicity.

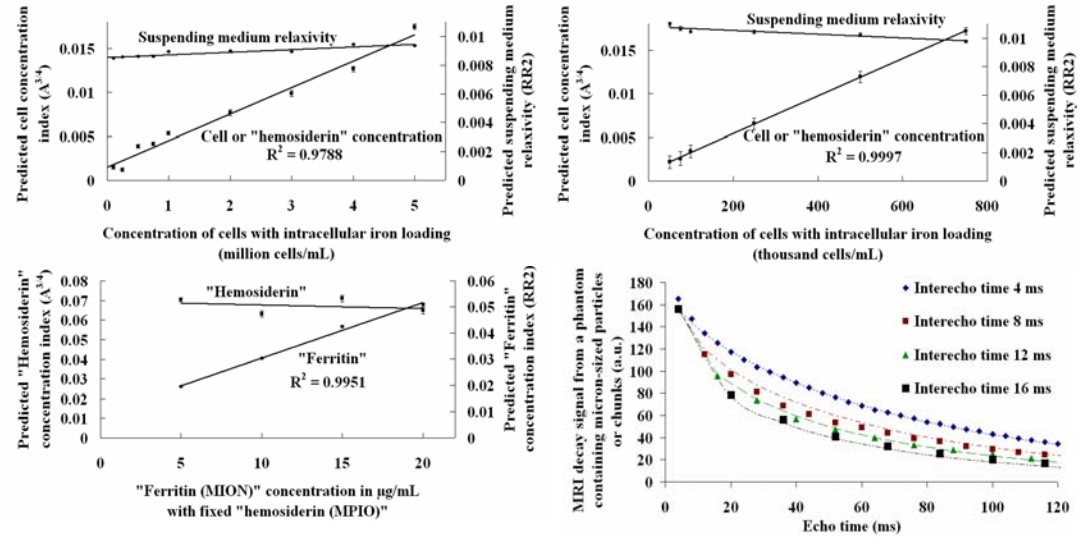


**Fig. 1** MRI estimates of iron in soluble and particulate mixture phantoms using a modified multi-echo CPMG sequence at 7 Tesla. **Top**: MRI estimation of the concentrations of mouse embryonic stem cells (ESCs) (top left) and human embryonic kidney cells (HEKs) (top right) suspended in agarose gel. The cells were intracellularly loaded with aggregated iron oxide particles (nanometer-sized MION particles for ESCs with 2-4 pg Fe/cell and 0.9 μm MPIO particles for HEKs with 3-10 pg/cell). **Bottom left**: MRI estimation of soluble nanometer-sized iron (MION, "ferritin") in varying concentrations with fixed concentration of micron-sized iron oxide particle concentration (4.5μm MPIO, $5x10^6$ beads/mL, "hemosiderin") in agarose gel phantoms. **Bottom Right**: Typical multi-echo CPMG signal decays with theoretical fittings from a phantom that contains micron-sized iron particles or chunks. Note these CPMG signal decays are non-exponential and have a strong dependence on the interecho time $2\Delta t$.

**REFERENCES** 1.Brittenham GM et al. Blood 2003;101(1):15. 2.Ghugre NR et al. MRM 2005;54(5):1185. 3.Jensen PD. Br J Haematol 2004;124(6):697. 4.Gossuin Y et al. MRM 2000;43(2):237. 5.Jensen JH et al. MRM 2002;47(6):1131. 6.Sheth S et al. Ann N Y Acad Sci 2005;1054:358.